

IMAGING OF SUBSURFACE TARGETS USING A 3D QUADTREE ALGORITHM

Ali Cafer Gürbüç, James H. McClellan and Waymond R. Scott Jr.

Georgia Institute of Technology
Atlanta, GA 30332-0250

ABSTRACT

The imaging of subsurface targets using Ground Penetrating Radar (GPR) is becoming an increasingly important area of research. Conventional image formation techniques expend large amounts of computation to fully resolve a region, even a region of clutter. However, by using multi-resolution techniques, e.g. quadtree algorithms, potential targets and clutter can be discriminated in a computationally efficient way. Prior work has focused on the development of 2D quadtree algorithms for surface targets. For mine detection, target depth adds another dimension; thus, we have developed a 3D quadtree algorithm, and applied a multi-stage detector that uses the energy change between quadtree stages to discriminate target and clutter regions. This algorithm is then tested on computer-generated data, as well as experimental data collected from a model mine field. Results show that target location information can be obtained even under near field and small aperture conditions.

1. INTRODUCTION

Synthetic aperture ground penetrating radar (GPR) techniques have been primarily used for imaging and detecting of subsurface targets. Other applications include the investigation of shallow geological and engineering features on land. In this paper, we consider the problem of detecting and imaging subsurface land mines. The ecologically desirable and non-destructive nature of GPR, as well as its capability of sensing variation in dielectric properties, makes GPR effective for the mine detection problem.

As the GPR antenna scans a region, the radar transmits and receives a series of pulses. The impulse response of such a synthetic aperture radar (SAR) is a spatially variant hyperbolic curve in the space-time domain. There are a variety of methods for combining the received echoes into an image; e.g. standard backprojection, or Fourier domain SAR image formation. All of these methods process the entire region of interest to make a detection decision. On the other hand, Quadtree backprojection is a multi-resolution

technique that uses a divide-and-conquer approach. At each stage, space-time imaging is first performed over a number of sub-patches separately. As the quadtree algorithm iterates, increasingly finer sub-patches of the scene are resolved. Detection of potential targets can be accomplished without fully resolving the entire scene. Thus, relative to standard backprojection, this method provides comparable results with increased computational efficiency.

Previous work has focused on developing quadtree algorithms for imaging surface targets. Subsurface target imaging adds a third dimension to the problem. Thus, we extend the quadtree approach to a three dimensional algorithm that handles volumes rather than surfaces. Quadtree methods are especially effective for far field and large aperture conditions; however, neither of the conditions exist in the mine detection problem. Nevertheless, results from computer-generated data, as well as experimental data measured at model mine fields at Georgia Institute of Technology, show that the 3D quadtree algorithm developed still provides useful target location information under these conditions.

In Section 2, the basic theory of backprojection and the 3D quadtree imaging/detection algorithm is presented. Synthetic and experimental data results are shown in Section 3.

2. BASIC THEORY

2.1. Standard Backprojection

Synthetic Aperture Radar (SAR) is an imaging technique in which the radar antenna is moved over the region being imaged to emulate a physically larger aperture. The recorded data consists of returned echo pulse sequences. Also a single return due to an ideal point-like reflector forms a hyperbolic contour in the space-time domain. The standard backprojection algorithm performs a coherent summation along all such hyperbolas for every pixel in the image. For 2D processing of an $N \times N$ image with N sensors, the algorithm performs $O(N^3)$ computations. For 3D processing of an $N \times N \times N$ volume with N^2 sensors, the computational complexity increases to $O(N^5)$. On the other hand, quadtree backprojection attains much more efficient results, requiring $N^2 \log N$ [1] computations for the 2D case, and

This work is supported under a MURI by the U.S. Army Research Office under contract number DAAD19-02-1-0252

$N^3 \log N$ for the 3D case.

2.2. 3D Quadtree Backprojection

The standard quadtree backprojection algorithm introduced by McCorkle [1] is basically a divide-and-conquer strategy that is a good approximation to standard backprojection. Instead of coherently summing over all aperture points, the quadtree divides the image into sub-patches and performs coherent summation over each of these sub-patches separately. Furthermore, the original (parent) sensors are combined to form new virtual (child) sensors. This is illustrated in Fig. 1 for the 2D case.

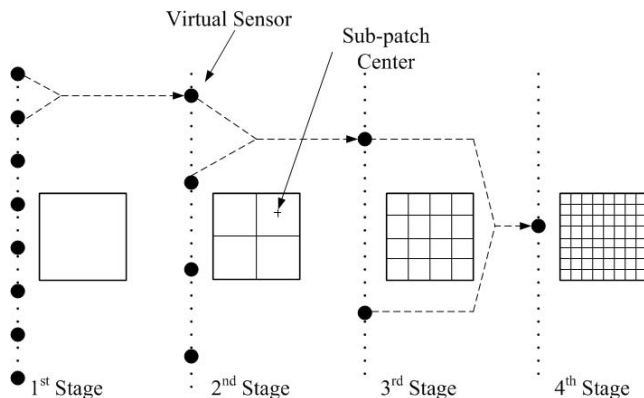


Fig. 1. Quadtree algorithm structure for the radix-2 case.

A similar partitioning is done by the 3D quadtree backprojection algorithm. In each iteration, the following operations are performed:

- *Partitioning of Imaged Region:* A volume is divided into $Q \times Q \times Q$ cubic sub-volumes. In the radix-2 case, this yields 8 sub-volumes. Because of this, the algorithm should be called an *oct-tree* but for imaging, the term quadtree is used to label this generic class of algorithms.
- *Combination of Parent Sensors:* Parent sensors are then combined to form one virtual sensor. There are many possible ways to group the parent sensors, and optimal selection methods have yet to be investigated. Nevertheless, as an initial choice, we decided to form a single virtual sensor from each $P \times P$ group of parent sensors. The location of the virtual sensor is then given by the coordinates of the center of the $P \times P$ square.
- *Child Sensor Data Regeneration:* Finally, an equivalent data stream must be derived from the measurements of the parent sensors. The portions of parent sensor data that correspond to time when the signal enters and leaves the sub-volume, are coherently

summed to form the child sensor data. The time at which the equivalent data segment begins or ends is determined by the travel time between the virtual sensor and the sub-volume. Thus, the calculation of these travel times is a critical part of the quadtree algorithm, and is discussed next.

Calculation of the signal travel times is depends on the distances between a parent sensor and the center of a sub-volume. To simplify the calculations, we first approximate the cubic sub-volume with a sphere encompassing the corners of the cube. Next, we consider the path traveled by the signal. In general, when an electromagnetic pulse encounters the boundary between two different media (such as air and soil), the propagation direction changes according to Snell's law. Taking wave refraction into account is especially critical for near-field imaging problems such as mine detection since the distance between antenna and target is relatively small. The exact calculation of the refraction point requires the solution of a 4th degree polynomial. We simplify the calculation by using an experimentally verified approximation [3], as illustrated in Fig.2:

$$x_2 \approx x_3 + \sqrt{\frac{\epsilon_1}{\epsilon_2}}(x_1 - x_3) \quad (1)$$

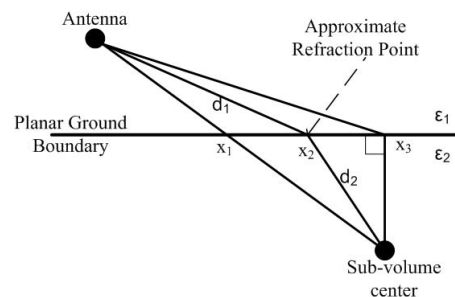


Fig. 2. Approximate refraction point determination

One-way travel times to the sub-volume are then found by dividing the calculated distances with wave velocity in air (c) and in ground (v) as follows:

$$t_{start} = \frac{d_1}{c} + \frac{d_2 - \Delta R}{v} \quad (2)$$

$$t_{stop} = \frac{d_1}{c} + \frac{d_2 + \Delta R}{v} \quad (3)$$

where ΔR is the radius of the spherical approximation of the sub-volume. It is important to note that the velocity of propagation in the ground is affected by the frequency of the wave, the type of soil, and the ground conductivity. A dry sand model ($\epsilon_2 = 4$) for the ground is chosen. It is assumed that the speed of the wave is constant throughout the ground.

The total energy in each sub-volume is defined as:

$$E_i(\xi, \eta, \kappa) = \sum_{s_x} \sum_{s_y} \sum_t |d(s_x, s_y, t, \xi, \eta, \kappa)|^2 \quad (4)$$

where ξ , η , and κ indicate the center coordinates of the sub-volumes; s_x and s_y indicate the spatial sensor position given a fixed elevation; and t represents the fast time.

By defining the intensity of each pixel as the energy for each sub-volume as shown in (4), a multi-resolution 3D image is obtained. The image of each quadtree stage is then scanned by a detection algorithm, as explained in the next section.

2.3. Detection and Region Elimination

The purpose of the detection is to distinguish regions containing coherent scatterers, such as mines, from other regions consisting of only clutter. The detector exploits the fact that from stage to stage, the energy for a coherent target increases relative to the total energy, while the energy of background noise and clutter decreases. Such energy differentials are exploited by defining a probability mass function (pmf) based on the ratio of the energy in a subvolume (s_{i+1}) to that in its parent (s_i):

$$P(s_{i+1}|s_i) = \frac{E(s_{i+1})}{E(s_i)} \quad (5)$$

The probability of a target being present at a subvolume in the stage $i+1$ is then given by Bayes Rule as

$$P(s_{i+1}) = P(s_{i+1}|s_i) \cdot P(s_i|s_{i-1}) \cdots P(s_1). \quad (6)$$

Thus, a probability for a target present is associated with every subvolume at the finest resolution of the quadtree. When no target is present, subsurface ground clutter measurements show that the noise is non-uniform. Nevertheless, for simplicity we used a Gaussian white noise approximation for the noise distribution. The generalized likelihood ratio test (GLRT) then takes the form

$$\frac{P(s_i)}{P_n(n)} \geq \gamma \quad (7)$$

where γ is a constant threshold.

3. EXPERIMENT AND RESULTS

3.1. Ground Reflection Elimination (GRE)

Reflection of the transmitted wave from the ground is a major obstacle in the imaging of subsurface targets. These reflections are higher in amplitude than any mine reflection and may result in unwanted artifacts in the focused image if it is not removed prior to signal processing. To eliminate

the ground reflection, first a model of the ground reflections is generated by averaging measurements of the ground reflection when no targets are present. This model is correlated with the returns at each measurement point to determine their relative lag. An appropriately delayed version of the model is then subtracted from the measurement. A line scan over two anti-personnel (AP) and one anti-tank (AT) mine is shown in Fig. 3 before and after GRE. Mine reflections can be seen clearer after GRE.

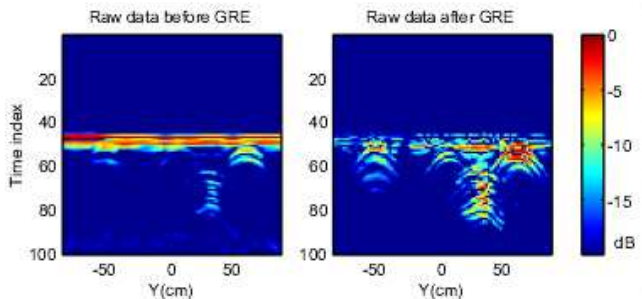


Fig. 3. Subsurface image before and after GRE.

3.2. Synthetic Data Results

We developed a GPR simulation program for the mine detection problem to test the algorithm on a variety of system configurations. System specifications such as aperture size, antenna height, the transmitter-receiver distance, target depth, and soil type, are all adjustable parameters. Here, we present the results for two synthetic data examples.

Example 1. In this scenario, two point reflectors in the sand are buried at positions (21, 4, -20) and (5, 27, -20). The system configuration is as follows: aperture size = 16; antenna height = 20 cm; transmitter-receiver distance = 5 cm; step size = 2cm; and soil type = dry sand with dielectric permittivity $\epsilon = 4$. Figure 4 shows an overhead view the result of the quadtree algorithm at different stages with the energy underneath the surface integrated to form the flattened images. Both targets are captured correctly by the algorithm and 92.2% of the surface area is eliminated from further investigation by other sensors or imaging algorithms. To give a sense of processing time advantage for this example quadtree method took 11.7s while brute force method took 110.6s to resolve the scene.

Example 2. A single target is placed at a position (13, 10, -10). All system parameters are the same as before, except that now the antenna height is 10 cm and the step size is 1 cm. Figure 5 shows the results with three-dimensional views. The target is twice as close as in the first example, yet 93% of the volume has been eliminated from further investigation.

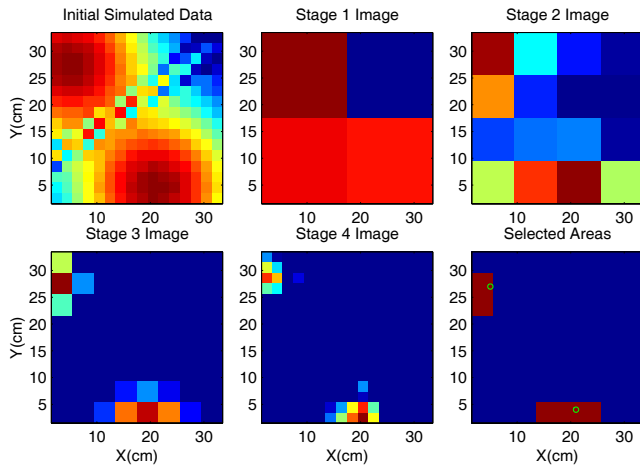


Fig. 4. Overhead view of results for synthetic data Ex. 1.

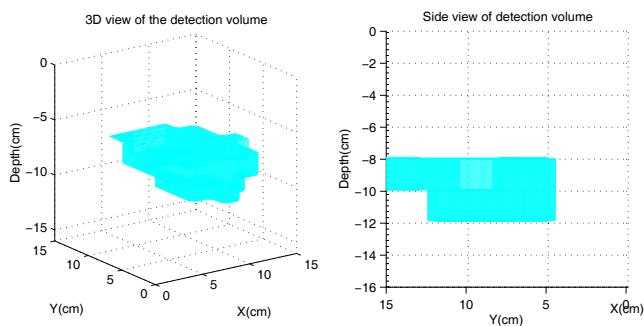


Fig. 5. 3D view of results for synthetic data Ex. 2.

3.3. Experimental Data Results

The 3D quadtree algorithm was tested in a model mine field at Georgia Institute of Technology using varying kinds of AP and AT mines as well as different sources of clutter, such as rocks and aluminum soft-drink cans. Figure 6 shows the quadtree algorithm applied on raw data measured over a VS-50 AP mine buried 1.3 cm deep. The height of the GPR transmitter and receiver is 11.43 cm, with a separation distance of 11.5 cm. With a step size of 2 cm, at this height the antennas have approximately a 16 point aperture length.

In this case, the object is very close to the ground; thus we are operating under low aperture size and very near-field conditions. Despite this, we were able to locate the mine and eliminate 87.5% of the region from consideration.

4. CONCLUSION

In this paper we have developed and verified the performance of a 3D quadtree backprojection algorithm for applications to the detection and imaging of subsurface landmines. Our results show that target location information can

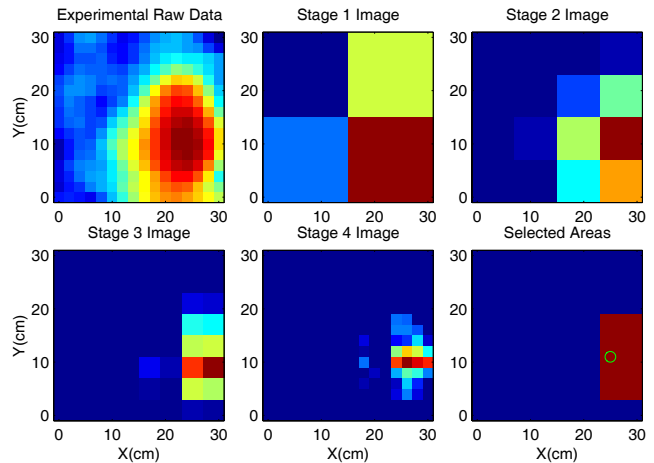


Fig. 6. Overhead view of experimental data results.

be extracted even under small aperture and near-field conditions. By applying a computationally efficient 3D quadtree algorithm, we have developed a fast GPR method to pre-screen a region and separate clutter from potential target locations. When additional, slower sensors (e.g., seismic sensors) are used in conjunction with GPR, the overall time requirements can be reduced by applying the slower sensors only to confirm the probable target regions identified by the quadtree algorithm. We plan to further pursue such sensor fusion issues in future work.

5. REFERENCES

- [1] J. McCorkle and M. Rofheart, "An order $n^2 \log n$ backprojector algorithm for focusing wide-angle wide-bandwidth arbitrary motion synthetic aperture radar," *Proc. of SPIE*, vol. 2747, pp. 25–36, 1996.
- [2] S-M. Oh, "Iterative space-time domain fast multiresolution SAR imaging algorithms," *Ph.D. Thesis, Georgia Institute of Technology*, 2001.
- [3] E. M. Johansson and J. E. Mast, "Three dimensional ground penetrating radar imaging using a synthetic aperture time-domain focusing," *Proc. of SPIE Conference on Advanced Microwave and Millimeter Wave Detectors*, vol. 2275, pp. 205–214, 1994.
- [4] L. M. Kaplan, J. H. McClellan and S-M. Oh, "Pre-screening During Image Formation for Ultrawideband Radar," *IEEE Trans. Aerospace and Electronic Systems*, vol. 38, no. 1, pp. 74–88, 2002.